PERGAMON

International Journal of Multiphase Flow 27 (2001) 737–752

International Journal of Multiphase Flow

www.elsevier.com/locate/ijmulflow

Brief communication

Dilute solid–liquid upward flows through a vertical annulus in a closed loop system

T.A. Özbelge *, A. Beyaz

Department of Chemical Engineering, Middle East Technical University, Ankara 06531, Turkey

Received 4 January 1999; received in revised form 30 July 2000

1. Introduction

In food and chemical industries, mining operations and wastewater treatment processes, solids may be conveyed in liquids through the conduits. Although there are many industrial applications of solid–liquid flows in technology, the available knowledge about particulate flows is not complete due to the difficulties encountered in analyzing these complex systems. Hydraulic transportation of solids in pipes has low operating and maintenance costs (Doron and Barnea, 1995) and therefore, it is a preferred method.

Sellgren (1982) discussed the two-phase pressure drops and the choice of operating velocities in the vertical upward pipe flows of solid–water mixtures. He reported that additional turbulence was created due to the relative velocity between the solid and fluid phases. Furuta et al. (1977) measured the radial local solid concentrations (RLSCs) in vertical upward and downward flowing suspensions through a vertical pipe. The radial solid profiles yielded a minimum at the pipe centre in the vertical upward flow of solid–water mixtures having solids heavier than water, and a maximum in the downward flow of the same mixtures. They claimed that the solid concentration profiles were smoothed over the cross-section of the pipe at very high flow Reynolds numbers of these mixtures. They also reported that the radial solid concentration profiles depended on density and size of the solid particles as well as the slurry velocity. An investigation of the phase distributions and the turbulent structure of solid–liquid upward flows in a vertical pipe was carried out by Alajbegoviç et al. (1994). They related the concentration distributions of solid particles heavier and lighter than water to the slip velocity, being a function of liquid flow rate and the density of solid material. Konno et al. (1981, 1979) investigated the heat transfer and flow characteristics of solid–liquid mixtures flowing upward or downward in a vertical pipe. They also observed the

* Corresponding author. Tel.: +90-312-210-2621; fax: +90-312-210-1264.
E-mail address: tozbelge@metu.edu.tr (T.A. Özbelge).

0301-9322/01/$ - see front matter
PII: S0301-9322(00)00047-1

distribution of particles in the pipe and reported that the ratio of transport solid concentration to the delivered solid concentration was greater than 1.0 for high relative velocities, but it approached to one at low relative velocities in view of the constant mass flow rate of solids. Since the circular pipe geometry is considered in most of the previous work (Ayukawa et al., 1980; Hsu et al., 1989; Ogawa et al., 1990), the data available for suspension flows in the other geometries is scarce (Sadatomi et al., 1982). The work by Hetsroni and Rozenblit (1994) is worth mentioning where they investigated heat transfer to a liquid–solid mixture in a flume by using infrared thermography technique effectively to study the thermal interaction between the particle-laden turbulent flow and a heated plate.

In practice, the annular geometry is encountered in many industrial applications such as double-pipe heat exchangers, nuclear reactor coolers, extruders, slurry transport reactors, fluidized beds and others. Therefore, the objective of this study is to obtain more experimental data in the annular geometry for better understanding of two-phase flow behaviour in this specific geometry. The flow characteristics of feldspar–water mixtures, flowing upward through a vertical annulus in a closed-loop system, is determined by measuring the radial concentration profiles of solids and the axial pressure drops in the test section, simultaneously. It is expected that the results of this study will be useful to explain the effect of solids on two-phase transport phenomena in the annular geometry (Özbelge and Köker, 1996).

2. Experimental

2.1. Experimental set-up

The set-up used in the experiments is shown in Fig. 1. It is a closed-loop system consisting of a centrifugal slurry pump with a by-pass line, horizontal and vertical lines made of galvanized iron, an orificemeter, a rotameter, a vertical annulus, a heat exchanger, a drain line and a feed-slurry tank. The vertical annulus made of steel is 500 cm high. Flared mixing chambers are placed at both ends of the annulus. At the entrance to the annulus, the mixing chamber having baffles ensures a homogeneous slurry feed to the annulus. Again at the exit of the annulus, a similar mixing chamber provides the uniform passage of slurry from the annulus to the upper horizontal pipe in the set-up. The inside diameter of the outer pipe (D_o) and the outside diameter of the inner pipe (D_i) being 12.5 and 2.5 cm, respectively, yield an aspect ratio $\kappa = D_i/D_o = 0.2$ and a hydraulic diameter $D_h = D_o - D_i = 10$ cm for the annulus. The distance from the bottom end of the annulus up to the test section (entrance length) is 225 cm, which provides a fully developed flow; the length of the test section is 200 cm. There are two pressure taps opposite to each other drilled in each cross-section at both ends of the test section. Two pressure transducers (Cole–Parmer, range: 0–15 psig) and a U-tube manometer connected to the test section, by means of these pressure taps, are used to measure the axial pressure drops.

The total pressure drop in the test section (frictional pressure drop + hydrostatic head) was measured by processing the signals from the transducers at a rate of 10 pressure readings per second in an IBM-PC via a programmed interface. At first, when the test section was completely full of water and the pump was not operating, the hydrostatic head in the test section was measured several times and an average value was obtained. Later the total pressure drops, in-

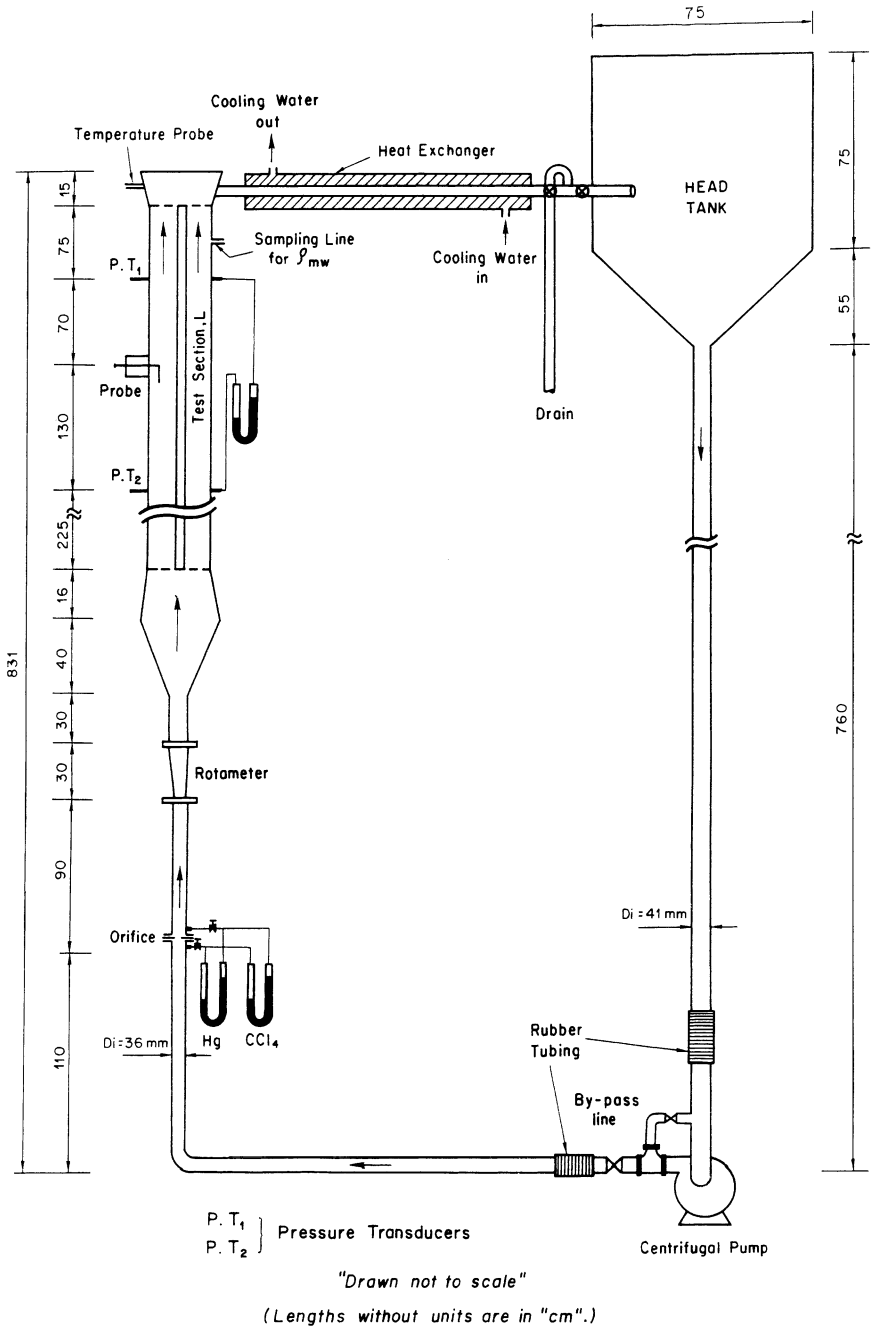

Fig. 1. The schematic diagram of the experimental set-up.

cluding the pressure drops due to flow besides the static head, were measured with the transducers at different water velocities. It was observed that the total pressure drops were not significantly different than the static head; since, the frictional pressure drops in single-phase (water) flows were

very small, it was not possible to measure them by means of the pressure transducers. Therefore, a U-tube manometer was used to measure the frictional pressure drops in the test section more accurately. This U-tube manometer, having a manometer fluid of CCl_4, was placed inclined at small angles to the horizontal. An inclination angle of 2°–10° provided the desired accuracy in small pressure drop measurements, especially those occurring in the laminar water flows without solids. In two-phase (feldspar–water) flow experiments, it was necessary to increase the inclination angle to 90° due to the greater pressure drops.

A sampling probe designed previously by Özbelge and Somer (1988) was used to measure the radial local solid concentrations (RLSCs) at a cross-section of the annulus perpendicular to the flow. The schematics of the probe is given in Fig. 2. The entire assembly of the sampling probe is tightly clamped on the annulus at a height of 130 cm from the beginning of the test section. The probe has an inner diameter of $D_{pi} = 0.2$ cm and an outer diameter of $D_{po} = 0.32$ cm. It could be traversed across the annular gap in the horizontal direction by a screw mechanism. The position of the probe-tip in the annular gap is followed on a scale by a needle. When the position of the probe-tip is changed, the distance travelled by the probe is read from a scale. The direction of the probe-tip is parallel to the streamlines of the flow as the tip-opening is facing the flow.

The flow rates are measured using an orificemeter mounted on the vertical pipe leading to the annulus; the orificemeter is placed away from the elbows to avoid the flow disturbances. It was calibrated with water. This calibration could not be repeated with the solid–liquid mixtures due to

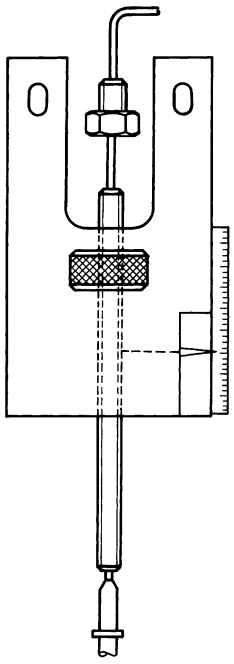

Fig. 2. The schematics of the sampling probe.

the limited amounts of solids and it was assumed that the error would not be significant in the case of very dilute solid–liquid mixtures used (Özbelge and Somer, 1988). A rotameter placed on the same vertical pipe in series with the orificemeter, was used to control the calibration of the orificemeter. In performing the experiments with feldspar–water flows, the rotameter was removed from the system to avoid the clogging in the system and not to cause additional resistance to flow. The flow rates lower than 40 l/min were measured with a CCl_4-manometer connected to the taps of the orificemeter and a Hg-manometer connected in parallel to the CCl_4-manometer, was used for the higher flow rates.

A cylindrical head tank made of stainless steel was used for the preparation of the feed slurry. The tank having a conical bottom to avoid the settling of the solids, is connected from its bottom to a centrifugal pump with a vertical pipe. The rubber tubings of about 20 cm long were used in connecting the pump to the set-up to eliminate the possible vibrations in the system during the operation of the pump (Fig. 1).

A heat exchanger, placed between the slurry tank and the top end of the annulus, maintains a constant slurry temperature during the flow experiments; the slurry would otherwise heat up during the circulation through the pump, in the closed-loop system. The slurry temperature was measured by a temperature probe and its digital meter (Cole–Parmer). The temperature-probe is inserted into the top mixing chamber at the exit of the annulus before the heat exchanger.

A short horizontal sampling line with a ball valve was constructed on the annulus-wall at a height of 30 cm from the exit end of the test section to determine the mixture density at the wall. In each experimental run, a sample of approximately 500 cm^3 was collected from this sampling port without diverting the whole flow through the annulus. From its measured volume and mass, the density of the mixture at the wall (ρ_{mw}) was determined.

The mixture is washed out of the system by a vertical drain-line, which is installed on the upper horizontal pipe, between the heat exchanger and the head tank. In cleaning the system, the ball valve before the drain line was opened and the other ball valve leading to the head tank was closed simultaneously. During this operation, the head tank was connected to an outside clean water source to avoid the emptying of the flow system. A representative solid sample for each particle size, was collected from the drain line to check the attrition of solids after the experiments, by a sieve analysis on the used particles. Five batches of feldspar particles ($K_2O{\cdot}Al_2O_3{\cdot}6SiO_2$) having mean particle diameters of 0.0064, 0.0115, 0.0138, 0.0165 and 0.0230 cm and a material density of $\rho_p = 2.4$ g/cm^3 were used in the experiments.

2.2. Experimental procedure

At the start of the experimental work, the orificemeter was calibrated with water using a Hg-manometer or a CCl_4-manometer as explained in Section 2.1. The pressure transducers were also calibrated. The transducers displayed 4 or 20 mA when zero or 15 psig was applied, respectively. The linearity between the pressure head in terms of pressure units of psi ($lb_f/in.^2$) and the pressure response of the transducers in terms of milliamperes was checked by observing the height of water level in the annulus by means of a vertical glass tube with a millimetric scale mounted on its side. When the pump was not operating and the system was full of water so as to wet both of the transducers, the heights of water columns over the transducers were measured from the scale connected to the glass tube, thus the gravity heads of water on each of the transducers were

calculated. At the same time, the pressure responses of the transducers were recorded in terms of milliamperes. This procedure was repeated by reducing the water level in the glass tube; it was observed that the calculated heads and the recorded milliamperes were linear. Thus, the calibration equations for the transducers were obtained (Beyaz, 1998).

Firstly, experiments with water were carried out to determine the accuracy of the present experimental set-up. Later, experiments with the solid–liquid mixtures were performed in a similar manner, as explained below.

The head tank was filled with water up to the marked level and the pump was started. Slurry, at a desired feed solid concentration (FSC) was prepared in the head tank by adding the weighed amount of uniformly sized feldspar particles at the chosen mean particle size. The mixture flow rate was adjusted manually by the valves using the calibration curve of the orificemeter. Afterwards, the flow rate of the cooling water to the heat exchanger was set. When the temperature of the mixture in the system remained constant with time, the simultaneous measurements of the axial pressure drops and the RLSCs were carried out in the test section. Also in each run, the mixture density at the wall was determined by taking a sample from the sampling port on the annulus-wall, without diverting the whole flow to the sampling line.

This procedure was repeated for different FSCs of each size of particles in water. At each FSC, experimental runs for different mixture velocities (in the range 0.8–19.3 cm/s) were performed. Altogether, 278 runs were performed with feldspar–water mixtures. In each of these runs, the frictional pressure drop in the test section and the mixture density at the wall were measured; but only in 152 runs, the radial solid concentration profiles were determined by the RLSC measurements (Beyaz, 1998). For each FSC, just before adjusting the slurry flow to a new velocity, the necessary amount of solids of that particle size and some water were added to the head tank to keep the liquid level the same and to compensate for the loss of material due to sampling. At the end of a day of experimentation, the solids were washed out of the system to prevent their settling in the pump, tank and pipes, and then the pump was turned off.

To measure the local solid concentrations (LSCs) at various points along the chosen diameter in the test cross-section, a gravimetric method was employed. A set of 50-ml Erlenmeyer flasks were washed, dried and weighed with their corresponding corks, to be used in the experiments. During the circulation of the slurry in the system, the samples of any volume (25–30 cm^3) passing through the sampling probe, were collected in 50 ml Erlenmeyer flasks. Each of these samples corresponded to a mixture of water and solids at a definite radial distance from the inner-pipe wall. This distance was read from the scale on the probe assembly. The Erlenmeyer flasks containing the collected samples were tightly closed with their corks just after the samples were taken, and were then weighed. These samples were carefully dried, preventing splashing, overnight in an oven at around 105°C. As soon as the flasks were removed from the oven, they were closed with their corresponding corks to avoid the absorption of moisture by the dried samples. They were cooled in a desicator and then weighed again with a sensitive balance to an accuracy of ±0.001 g. Thus, the RLSC at each radial distance was calculated. The scope of the experiments is given in Table 1.

In Table 1, the mixture Reynolds number is defined as, $Re_m = D_h\ U_{ann}\ \bar{\rho}_m/\bar{\mu}_m$ where D_h is the hydraulic diameter, U_{ann} the velocity in the annulus, $\bar{\rho}_m$ the average transport mixture density (ATMD) in the test section and $\bar{\mu}_m$ is the average viscosity of the mixture calculated from Eq. (1) (Kofanov, 1964):

Table 1
The ranges of experimental parameters in flow experiments

Solid concentration in feed slurry, C_f (% v/v)	0.3–2.3
Solid particle size, d_p (cm)	0.0064–0.0230
Reynolds number of the mixture, $Re_m = D_h\ U_{ann}\ \bar{\rho}_m/\bar{\mu}_m$	800–20000
Mixture velocity in the annulus, U_{ann} (cm/s)	0.8–19.3

$$\bar{\mu}_m = \mu_w(1 + 2.5 * \bar{\phi}_s). \quad (1)$$

In Eq. (1), μ_w is the viscosity of water at the measured temperature of the mixture in each experimental run and $\bar{\phi}_s$ is the average volume fraction of solids in the test cross-section of the annulus. The calculation of $\bar{\phi}_s$ is explained in the next section.

3. Results and discussion

Hydrodynamic characteristics of single-phase flows (laminar, transition and turbulent flow regimes) are known well, but the same is not valid for two-phase and multi-phase flows. Therefore, in this study, the flow characteristics of feldspar–water mixtures is investigated experimentally at the steady state; the relationship between the axial two-phase frictional pressure drops and the radial concentration distributions of solids in the test section is determined for the vertical upward flows of these mixtures in a concentric annulus at different operating conditions.

The experimental results obtained with single-phase water flows were compared with the theoretical ones calculated from the well-known equations of fluid-mechanics (McCabe et al., 1985) to check the accuracy of the present experimental set-up. These are given elsewhere (Özbelge and Beyaz, 1999). The repeated runs show that the uncertainty in the frictional pressure drop measurements is ±2%.

3.1. Feldspar–water flow experiments in the vertical annulus

The most important characteristic of two-phase flows is known to be the pressure drop versus mixture velocity relationship. Since the flow is vertical upward, the effect of the hydrostatic head must be considered. The two-phase frictional pressure drops (ΔP_{tp}) are calculated from Eq. (2) at different mixture velocities,

$$\Delta P_{tp} = hg(\rho_{CCl4} - \bar{\rho}_m), \quad (2)$$

where, h is the U-tube manometer reading, $\bar{\rho}_m$ average mixture density obtained from the RLSC measurements in the test cross-section during the flow as explained later in this section, ρ_{CCl4} is the density of manometer liquid and g is the gravitational acceleration. Using $\bar{\rho}_m$ in Eq. (2) may be questionable thinking that the tubings of the manometer will be clogged if they are filled with the solid–liquid mixture; but considering that the slurry contains micron-size particles at very low concentrations and observing the turbid water in the manometer tubings, it will not be correct to use the density of water (ρ_w) instead of $\bar{\rho}_m$ in Eq. (2). The validity of this argument was checked with the Bernoulli equation written between the entrance and exit planes of the test section (Özbelge and Beyaz, 1999). If the tubings of the manometer were filled with water, the application

of the Bernoulli equation with the present experimental data would yield negative values for ΔP_{tp} in the test section. This is not realistic which shows that the last hypothesis is not acceptable; in other words, the tubings of the manometer connected to the test section are filled with the dilute feldspar–water mixture rather than water.

ΔP_{tp} values can also be calculated according to Eq. (3) from the total pressure drop (ΔP_{total}) values obtained with the pressure transducers:

$$\Delta P_{tp} = \Delta P_{total} - \bar{\rho}_m g L. \tag{3}$$

The ΔP_{tp} values from Eq. (2) are in agreement with those calculated from Eq. (3) within an error margin of ±6%, the latter being less reliable; because in Eq. (3), the greater magnitude of the static head term ($\bar{\rho}_m$ g L) compared to the frictional two-phase pressure drop (ΔP_{tp}) causes a reduction in the accuracy of the calculations. Therefore, the ΔP_{tp} values calculated from Eq. (2) are presented in this paper (see Figs. 3–5) and ΔP_{total} values are not reported here. The average transport mixture density (ATMD), $\bar{\rho}_m$, appearing in Eqs. (2) and (3) is calculated from Eq. (4) where $\bar{\rho}_s$ is the average solid density (ASD) over the flow area in the test cross-section obtained

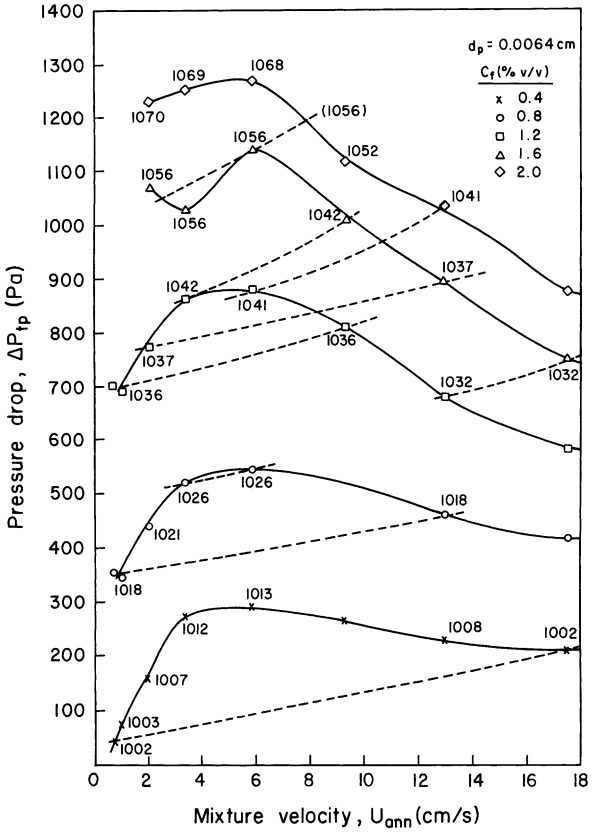

Fig. 3. Two-phase frictional pressure drop versus mixture velocity, at different $\bar{\rho}_m$ in the test section and at different C_f, for $d_p = 0.0064$ cm.

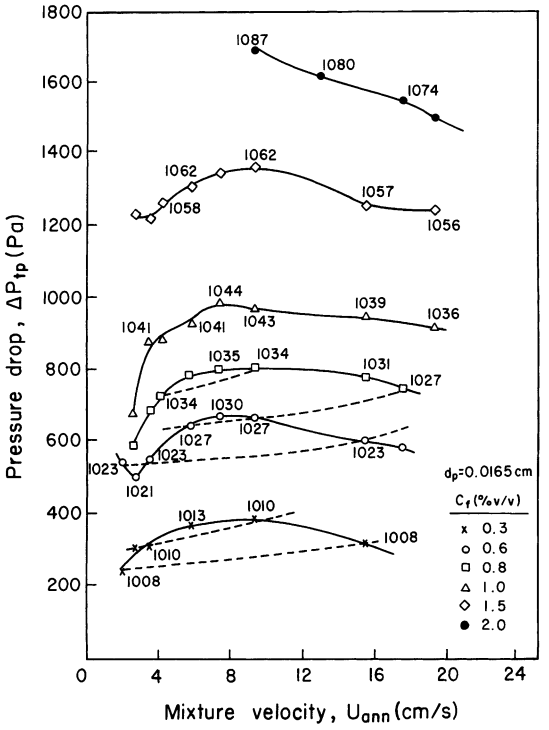

Fig. 4. Two-phase frictional pressure drop versus mixture velocity, at different $\bar{\rho}_m$ in the test section and at different C_f, for $d_p = 0.0165$ cm.

from Eq. (5) by graphical integration of the local solid density versus radial distance data, R_i and R_o being the radii of the inner and outer pipes, respectively.

$$\bar{\rho}_m = \bar{\rho}_s + (1 - \bar{\phi}_s)\rho_w, \tag{4}$$

where $\bar{\phi}_s$ is the average volume fraction of solids (volume of solids/volume of mixture, v/v) at the test cross-section of the annulus, being equal to $(\bar{\rho}_s/\rho_p)$.

$$\bar{\rho}_s = \frac{\int_{R_i}^{R_o} \rho_s 2\pi r \, dr}{\pi(R_o^2 - R_i^2)}, \tag{5}$$

where ρ_s is a function of r. For each experimental run, the ASD $(\bar{\rho}_s)$ is obtained from Eq. (5) and used to calculate the average $\bar{\phi}_s$ (v/v) value from $\bar{\rho}_s/\rho_p$. Thus $\bar{\rho}_m$ and $\bar{\mu}_m$ values are calculated from Eqs. (4) and (1), respectively. Using the whole experimental data, the calculated $\bar{\rho}_s, \bar{\rho}_m$ and $\bar{\phi}_s$ values are given elsewhere (Özbelge and Beyaz, 1999). The average solid concentration ($\bar{C}_s$ in terms of % v/v) is obtained from Eq. (6) where ρ_p is the material density of feldspar particles.

$$\bar{C}_s = (\bar{\rho}_s/\rho_p) \times 100 = \bar{\phi}_s \times 100. \tag{6}$$

From the repeated runs, the uncertainty in the LSC measurements is found to be ±2%. The concentration probe used in the determination of the RLSCs is the same one which had been designed and successfully used in the previous study by Özbelge and Somer (1988), giving results

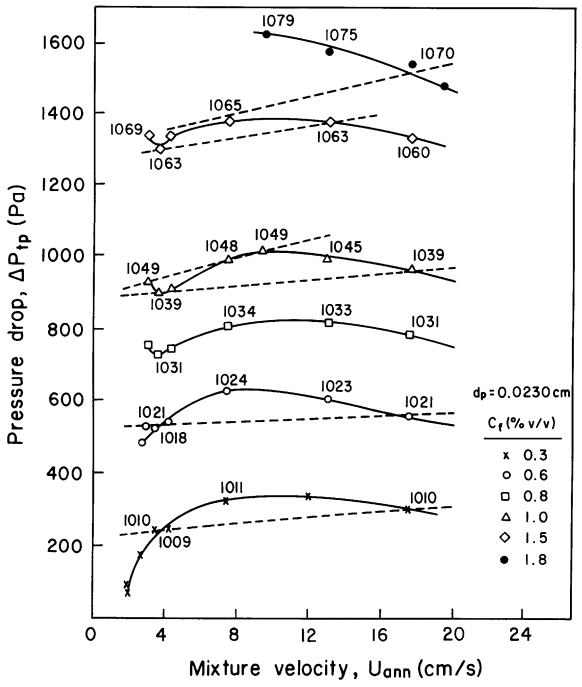

Fig. 5. Two-phase frictional pressure drop versus mixture velocity, at different $\bar{\rho}_m$ in the test section and at different C_f, for $d_p = 0.0230$ cm.

in good agreement with the literature (Toda et al.,1972). In each experiment, the mixture density measured at the wall (ρ_{mw}) is compared with the ATMD ($\bar{\rho}_m$) in the test cross-section obtained from Eq. (4). The maximum percentage difference between the two values (ρ_{mw} and $\bar{\rho}_m$) is $\pm 1\%$, which indicates the reliability of the local solid density (concentration) measurements with the sampling-probe. The distance between the locations of the sampling probe used to measure the radial local solid densities and the sampling port used for the wall sampling is around 100 cm (Fig. 1), which shows that the ATMD does not significantly change with the height of the annulus.

For feldspar–water flows at different operating conditions, the experimental and the calculated parameters are tabulated elsewhere (Özbelge and Beyaz, 1999), the experimental parameters being the particle size (d_p), feed solid concentration (C_f), mixture velocity in the annulus (U_{ann}), manometer reading (h) and the calculated parameters being the two-phase frictional pressure drops (ΔP_{tp}), the average transport mixture density ($\bar{\rho}_m$), the average solid-phase density ($\bar{\rho}_s$) and the average volume fraction of solids ($\bar{\phi}_s$) in the test section.

The feed solid concentration (C_f) being a parameter, the ΔP_{tp} values versus the mixture velocities are shown in Figs. 3–5, for the mean particle sizes of 0.0064, 0.0165 and 0.0230 cm. In these figures, each curve corresponds to a specific C_f of that particle size, and the values written on the curves indicate the ATMD values (in kg/m^3) calculated from Eq. (4) for each experiment at a different mixture velocity. The same values of the ATMD attained in the test section, which may correspond to different operating conditions (different mixture velocities and feed solid concentrations) of the feldspar–water flows for a specific particle size, are joined to get the iso-ATMD

lines. On these dotted lines where the ATMD is constant, it is observed in Figs. 3–5 that the ΔP_{tp} increases with the increasing mixture velocity. This is an expected result (McCabe et al., 1985). As seen from Figs. 3–5, the ΔP_{tp} increases with C_f for each particle size, at the same mixture velocity. It also increases with the increasing particle size, keeping the C_f and the mixture velocity constant. Depending on the characteristics of the system, each (ΔP_{tp} versus mixture velocity) curve passes through a peak-ΔP_{tp} value at a certain mixture velocity. The peak value of ΔP_{tp} occurs when the ATMD reaches its peak value for a specific FSC of that particle size. For the same FSC, the peak value of the ΔP_{tp} and that of the ATMD occur almost at the same mixture velocity. First increasing behaviour of ATMD in the test section with the mixture velocity and then a decrease in ATMD with a further increase in the mixture velocity, at constant FSC, can be explained with the following arguments.

At very low mixture velocities, some of the particles may settle down in the horizontal pipe section before the annulus, forming a fixed or a moving bed due to the size distribution of the feldspar particles. Therefore, the amount of solids carried to the vertical annulus will be less. The amount of solids carried to the annulus will gradually increase with the increasing mixture velocity due to the decrease in the amount of settled solids in the horizontal pipe section. As a result, the ATMD in the test section increases with the increasing mixture velocity and reaches its peak value in the test section when there is no solid settled in the horizontal section and almost all the solids are in suspension. With further increase in the mixture velocity, the ATMD in the test section decreases due to the more homogeneous distribution of the whole solids added to the head tank in the preparation of the feed slurry, to the overall system.

The repeated runs show that ±2.5% error in the mixture velocity measurements and ±2% error in the ΔP_{tp} measurements occur in the feldspar–water flow experiments. The sieve analyses of the feldspar particles before and after the experiments indicate that the attrition of the solids is not significant during the circulation of the solid–liquid mixtures in the closed-loop system for a day of experimentation. Nevertheless, the used solids were discarded and not used again.

3.2. Radial solid concentration profiles in the vertical annulus

The determination of the phase distributions in two-phase flows has been a challenge due to the difficulties of the experimental work in these systems. Especially in the annular geometry, the interactions between the phases and their effects on heat and mass transfer phenomena could not be explained properly (Özbelge and Köker, 1996). In the present study, the RLSCs are measured for the feldspar–water mixtures flowing upward in a vertical concentric annulus at different operating conditions. The figures representing some of the data are reported here and the rest of the data is given elsewhere (Beyaz, 1998; Özbelge and Beyaz, 1999). At different FSCs of each particle size, the local solid concentrations (C_s, % v/v) versus the radial distance (r, cm) are plotted in Figs. 6–10, the mixture Reynolds number (Re_m) being a parameter. In these figures, the radial distance is measured from the centre of the concentric pipes to the point where the LSC measurement is made in the test cross-section. As observed in Fig. 6, the LSCs do not show considerable variation with the radial distance for very dilute slurries ($C_f = 0.4\%$ v/v) containing very small particles ($d_p = 0.0064$ cm), and therefore, the radial solid concentration profiles are almost uniform at each Re_m. The RLSCs increase in the test section with the increasing mixture velocity (or the Re_m) up to a certain velocity and then they decrease again with the increasing velocity or

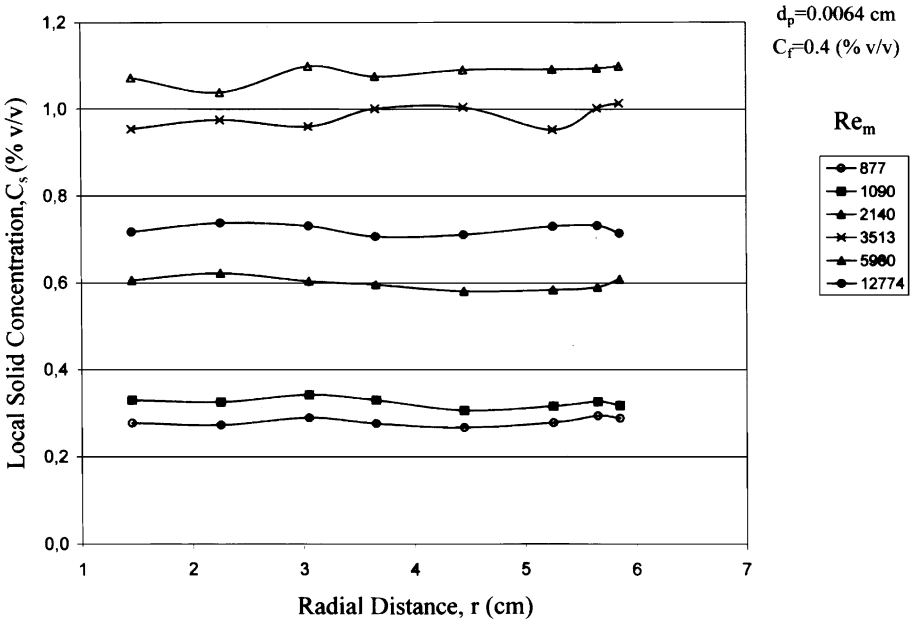

Fig. 6. Local solid concentration in the test cross-section as a function of radial distance at different mixture velocities for feldspar particles of $d_p = 0.0064$ cm, at $C_f = 0.4\%$ v/v.

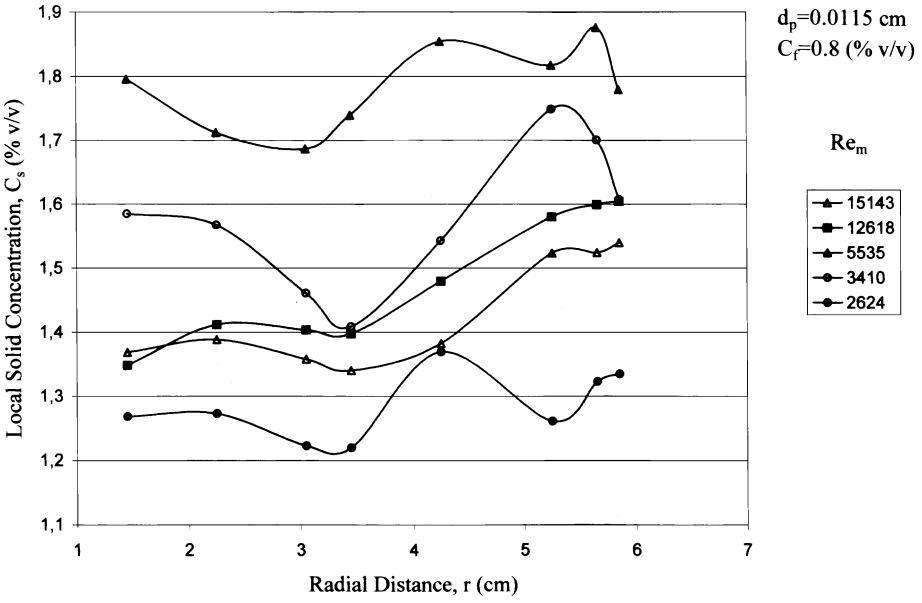

Fig. 7. Local solid concentration in the test cross-section as a function of radial distance at different mixture velocities for feldspar particles of $d_p = 0.0115$ cm, at $C_f = 0.8\%$ v/v.

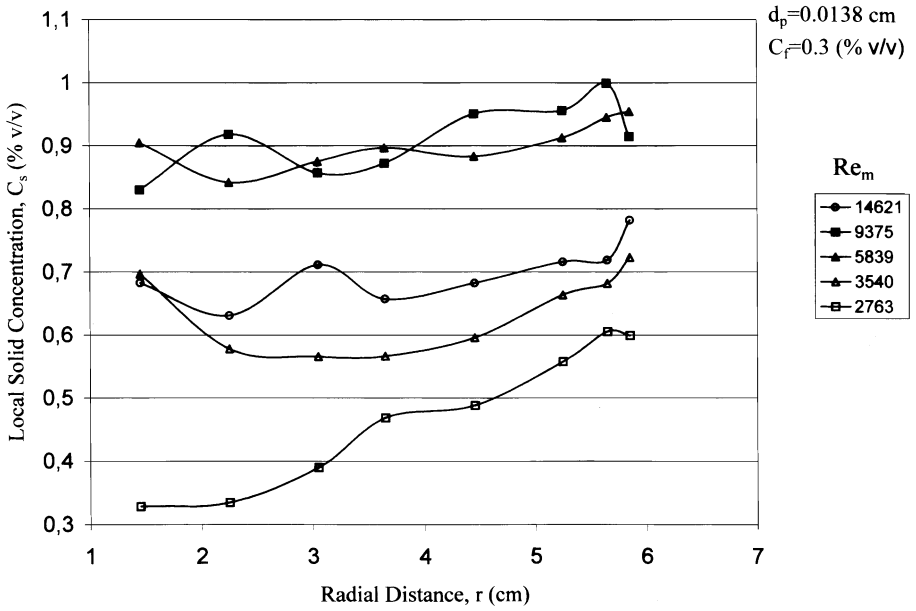

Fig. 8. Local solid concentration in the test cross-section as a function of radial distance at different mixture velocities for feldspar particles of $d_p = 0.0138$ cm, at $C_f = 0.3\%$ v/v.

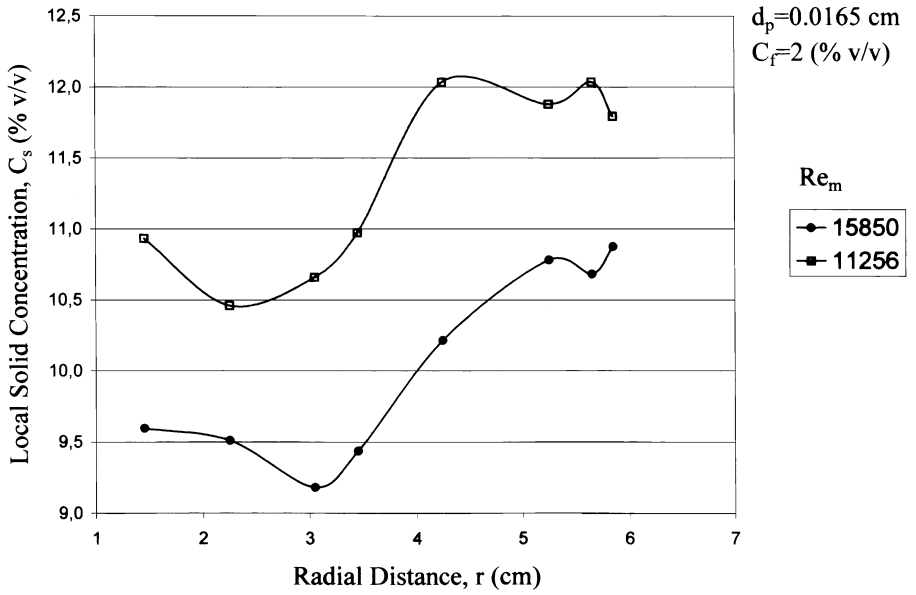

Fig. 9. Local solid concentration in the test cross-section as a function of radial distance at different mixture velocities for feldspar particles of $d_p = 0.0165$ cm, at $C_f = 2.0\%$ v/v.

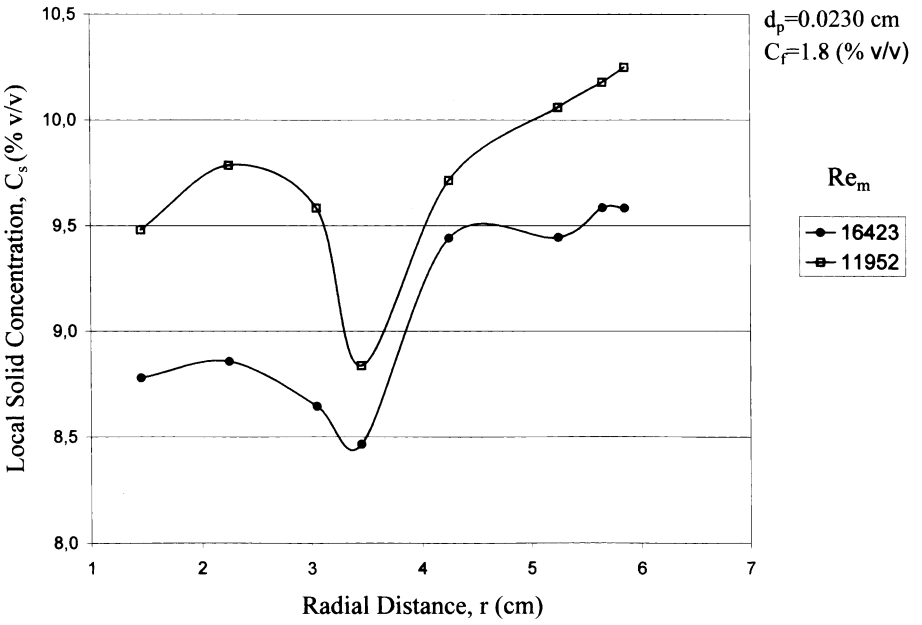

Fig. 10. Local solid concentration in the test cross-section as a function of radial distance at different mixture velocities for feldspar particles of $d_p = 0.0230$ cm, at $C_f = 1.8\%$ v/v.

the increasing mixture Reynolds number, depending on the characteristics of the system as explained in Section 3.1.

The solid phase shows its effect yielding the radial solid concentration profiles in different shapes with increasing particle size and C_f (Figs. 7–10). After considering all the radial solid concentration profiles (Beyaz, 1998) obtained in this work at different experimental conditions, it can be concluded that generally the values of LSC are higher near the outer wall compared to those near the inner wall of the annulus. Also, a slight minimum seems to occur at a dimensionless radial distance ($\lambda = r/R_o$) within the range $0.35 \leqslant \lambda \leqslant 0.55$ in the Re_m range 800–20 000; the solid concentration profiles suggest that the radial location of this minimum solid concentration is most probably determined by the combined effects of the particle size, FSC and the Re_m in each experiment.

In single phase laminar flow through an annulus with the same aspect ratio as that of the annulus used in this work, namely $\kappa = 0.2$, the dimensionless radial distance of $\lambda = 0.546$ is calculated from Eq. (7) (Bird et al., 1960) where the shear stress is zero and the point velocity is maximum.

$$\lambda = (1 - \kappa^2)^{0.5} / (2 \ln (1/\kappa))^{0.5}. \tag{7}$$

With the available data, it is not possible to say whether the minimum point of the radial solid concentration profile and the maximum point of the velocity profile occur at the same dimensionless radial distance or not. Since the velocity profiles of the phases have not been measured in the present study, this point remains unresolved and needs further work to clarify how the solid concentration is affected by the two-phase velocity or vice versa.

4. Conclusions

The steady laminar and turbulent upward flows of feldspar–water mixtures through a vertical annulus (aspect ratio of $D_i/D_o = 0.2$ and a hydraulic diameter of $D_o - D_i = 10$ cm) are studied experimentally. (L_e/D_h), the distance of the entrance length to the test section divided by the hydraulic diameter, being an important parameter to provide a fully developed flow, is 22.5 in pressure drop measurements and 35.5 in local solid concentration measurements. The conclusions derived from this study are given below:

- The two-phase pressure drop (ΔP_{tp}) increases with the feed solid concentration (FSC) of each particle size, at the same mixture velocity. The ΔP_{tp} also increases with the increasing particle size keeping the FSC and the mixture velocity constant.
- The same values of the average transport mixture density (ATMD) attained in the test section, may correspond to different operating conditions (different mixture velocities and FSCs) of the feldspar–water flows for a specific particle size, are joined to get the iso-ATMD lines. At the same ATMD in the test section, the axial two-phase frictional pressure drop increases with the increasing mixture velocity.
- Depending on the characteristics of the system, the peak values of the ATMD and ΔP_{tp} occur almost at the same mixture velocity, the value of which may vary with the FSC chosen in the experiments for each particle size.
- The local solid concentrations (LSCs) do not show considerable changes in the radial direction for the conditions of very small particle sizes (e.g., 0.0064 cm) at very low FSCs (e.g., 0.4% v/v) in feldspar–water upward flows. From the radial solid concentration profiles, it can be concluded that generally the values of LSC are higher near the outer wall compared to those near the inner wall of the annulus. Also, a slight minimum seems to occur at a dimensionless radial distance ($\lambda = r/R_o$) within the range $0.35 \leqslant \lambda \leqslant 0.55$ in the mixture Reynolds number (Re_m) range 800–20 000; with the available data, it is not possible to say whether or not the minimum point of the radial solid concentration profile and the maximum point of the velocity profile occur at the same dimensionless radial distance.

Acknowledgements

This work was financed by the Scientific and Technical Research Council of Turkey (TÜBİTAK; Project No: İNTAG-822) and partially by the Middle East Technical University. The authors express their appreciation for these supports.

References

Alajbegoviç, A., Assad, A., Bonetto, F., Lahey, R.T., 1994. Phase distribution and turbulence structure for solid–liquid upflow in a pipe. Int. J. Multiphase Flow 20, 453–479.

Ayukawa, K., Kataoka, H., Hirano, M., 1980. Concentration profile, velocity profile and pressure drop in upward solid–liquid flow through a vertical pipe. BHRA Fluid Engineering Paper E2, p. 195–201.

Beyaz, A. 1998. Flow Characteristics of Dilute Solid–liquid Upward Flows in a Vertical Annulus, M.Sc. Thesis, Middle East Technical University, Ankara.

Bird, R.B., Stewart, W.E., Lightfoot, E.N., 1960. Transport Phenomena. Wiley, New York.

Doron, P., Barnea, D., 1995. Pressure drop and limit deposit velocity for solid–liquid flow in pipes. Int. J. Multiphase Flow 50, 1595–1604.

Furuta, T., Tsujimoto, S., Toshima, M., Okazaki, M., Toei, R., 1977. Concentration distribution of particles in solid–liquid two-phase flow through vertical pipe. Kagaku Kogaku Ronbunshu 4, 605–615.

Hetsroni, G., Rozenblit, R., 1994. Heat transfer to a liquid–solid mixture in a flume. Int. J. Multiphase Flow 20, 671–689.

Hsu, L.F., Turian, M.R., Ma, T., 1989. Flow of noncolloidal slurries in pipelines. AIChE J. 35, 429–441.

Kofanov, V.J., 1964. Heat transfer and hydraulic resistance in flowing liquid suspension in pipes. Int. Chem. Eng. 4, 426–430.

Konno, H., Harada, E., Toda, M., Kuriyama, M., Saruta, S., 1981. Heat transfer characteristics of solid–liquid upward flow through vertical pipes. Kagaku Kogaku Ronbunshu 6 (3), 308–311.

Konno, H., Harada, E., Toda, M., Kuriyama, M., Asano, M., 1979. Heat transfer of solid–liquid mixtures in vertical downward flow. Kagaku Kogaku Ronbunshu 5 (5), 464–470.

McCabe, W.L., Smith, J.C., Harriot, P., 1985. Unit Operations of Chemical Engineering. McGraw-Hill, New York.

Ogawa, K., Yoshikawa, S., Suguro, A., Ikeda, J., Ogawa, H., 1990. Flow characteristics and circular pipe flow of pulp suspension. J. Chem. Eng. Japan 123, 1–6.

Özbelge, T.A., Somer, T.G., 1988. Hydrodynamic and heat transfer characteristics of liquid–solid suspensions in horizontal turbulent pipe flow. Chem. Eng. J. 38, 111–122.

Özbelge, T.A., Köker, S.H., 1996. Heat transfer enhancement in water–feldspar upflows through vertical annuli. Int. J. Heat Mass Transfer 39, 135–147.

Özbelge, T.A., Beyaz, A., 1999. Seyreltik Sıvı-Katı Karışımlarının Akış Özellikleri. Project Report No: 196 I 010, Project No.: İNTAG-822, TÜBİTAK, Ankara, Turkey.

Sadatomi, M., Sato, Y., Saruwatari, S., 1982. Two-phase flow in vertical noncircular channels. Int. J. Multiphase Flow 8, 641–655.

Sellgren, A., 1982. The choice of operating velocity in vertical solid–water pipeline systems. BHRA Fluid Eng., Paper D3, 211–226.

Toda, M., Shimizu, T., Saito, S., Maeda, S., 1972. In: Preprint for 37th Annual Meeting of Society of Chemical Engineers, Japan, B-310.